NeuroImage 221 (2020) 117151

Contents lists available at ScienceDirect

NeuroImage

journal homepage: www.elsevier.com/locate/neuroimage

Pinpointing the optimal spatial frequency range for automatic neural facial fear processing

Stephanie Van der Donck[a,b,*,1], Tiffany Tang[a,1], Milena Dzhelyova[c], Johan Wagemans[b,d], Bart Boets[a,b]

[a] Center for Developmental Psychiatry, Department of Neurosciences, KU Leuven, Leuven, Belgium
[b] Leuven Autism Research (LAuRes), KU Leuven, Leuven, Belgium
[c] Institute of Research in Psychological Sciences, Institute of Neuroscience, Université de Louvain, Louvain-La-Neuve, Belgium
[d] Brain and Cognition, KU Leuven, Belgium

ARTICLE INFO

Keywords:
EEG
FPVS
Facial emotion processing
Implicit fear detection
Spatial frequency

ABSTRACT

Faces convey an assortment of emotional information via low and high spatial frequencies (LSFs and HSFs). However, there is no consensus on the role of particular spatial frequency (SF) information during facial fear processing. Comparison across studies is hampered by the high variability in cut-off values for demarcating the SF spectrum and by differences in task demands. We investigated which SF information is minimally required to rapidly detect briefly presented fearful faces in an implicit and automatic manner, by sweeping through an entire SF range without constraints of predefined cut-offs for LSFs and HSFs. We combined fast periodic visual stimulation with electroencephalography. We presented neutral faces at 6 Hz, periodically interleaved every 5th image with a fearful face, allowing us to quantify an objective neural index of fear discrimination at exactly 1.2 Hz. We started from a stimulus containing either only very low or very high SFs and gradually increased the SF content by adding higher or lower SF information, respectively, to reach the full SF spectrum over the course of 70 s. We found that faces require at least SF information higher than 5.93 cycles per image (cpi) to implicitly differentiate fearful from neutral faces. However, exclusive HSF faces, even in a restricted SF range between 94.82 and 189.63 cpi already carry the critical information to extract the emotional expression of the faces.

1. Introduction

Human faces contain a large and varied set of sources of information, conveyed by a spectrum of spatial frequencies (SFs) – i.e. the basic components of visual information, characterized by their spatial distribution of luminance variations (De Valois and De Valois, 1980). This information needs to be extracted fast and efficiently during social interaction in order to be able to act appropriately in every situation (Ruiz-Soler and Beltran, 2006). It has been suggested that the information represented by the various SFs in a face is processed in a coarse-to-fine sequence: the coarse and more global low SF (LSF) information is being processed first, with subsequent processing of the fine and more local higher SFs (HSF), for robust and precise categorization (De Cesarei and Codispoti, 2013; Goffaux et al., 2011; Goffaux and Rossion, 2006; Hegdé, 2008; Quek et al., 2018). However, other authors have argued in favour of a more flexible use of spatial frequencies rather than a fixed one, based on task demands and stimulus properties (de Gardelle and Kouider, 2010; Morrison and Schyns, 2001; Ruiz-Soler and Beltran, 2006; Schyns and Oliva, 1999).

To better understand how the visual system processes faces, several studies have aimed at pinpointing the range of SFs that play the most crucial role in (different aspects of) face processing. Very roughly, SFs < 8cpi can be considered as LSFs, 8 cpi < SFs < 24 cpi as middle-range SFs (MSFs), and SFs > 24 cpi as HSFs (Morrison and Schyns, 2001; Schyns and Oliva, 1999; Vuilleumier et al., 2003; Wang et al., 2015). Some studies emphasize the importance of LSF information for face discrimination or face recognition, suggesting the redundancy of HSF information (Canário et al., 2016; Goffaux et al., 2003a). On the other hand, the importance of both LSF and HSF information for face recognition has also been reported (Fiorentini et al., 1983; Flevaris et al., 2008; Halit et al., 2006). Finally, while either LSFs or HSFs may enable face recognition, the optimal SF range for face recognition has been suggested to comprise

* Corresponding author. Kapucijnenvoer 7 blok h - box 7001, 3000, Leuven, Belgium.
E-mail address: stephanie.vanderdonck@kuleuven.be (S. Van der Donck).
[1] Indicates shared first authorship.

https://doi.org/10.1016/j.neuroimage.2020.117151
Received 21 January 2020; Received in revised form 2 June 2020; Accepted 5 July 2020
Available online 13 July 2020

MSFs (Collin et al., 2012; Costen et al., 1996; Leonard et al., 2010; Morrison and Schyns, 2001; Ruiz-Soler and Beltran, 2006). This particular tuning of the visual system towards MSFs for face processing, may align with the fact that most physical face information is present in this MSF range, with facial amplitude maxima occurring around 10 cpf, particularly in horizontal orientation (Collin et al., 2014; Keil, 2008).

1.1. Spatial frequencies and emotional face perception

In addition to identity information, faces can also convey an assortment of emotional information. Compared to facial identity recognition, facial emotion recognition requires more details (Gao and Maurer, 2011) and has a greater sensitivity to changes in SF (Goren and Wilson, 2006). Depending on the displayed facial expression, different SF information is preferentially used during processing. For example, when categorizing fearful versus neutral expressions, a LSF bias has been observed, both at the behavioural (Holmes et al., 2005) and at a neural level (Pourtois et al., 2005; Vlamings et al., 2009; Vuilleumier et al., 2003). The LSF bias for behavioural fear categorization has also been demonstrated when compared to faces displaying happiness (Morawetz et al., 2011). However, other studies reported an advantage of HSF information for the detection of fearful versus neutral faces (Stein et al., 2014), and the recognition of fear as opposed to other facial expressions, including anger, happiness and disgust (Smith and Merlusca, 2014). Moreover, as for identity perception, the importance of MSFs has also been demonstrated for expression recognition (Gao and Maurer, 2011).

Overall, and irrespective of the particular emotion being presented, conflicting results have been found on the role of SFs in emotional face processing (for reviews, see De Cesarei and Codispoti, 2013; Jeantet et al., 2018). The methodological variability across studies, in terms of the emotion processes being measured, the methods to modulate the SF availability at the stimulus level, and the experimental parameters (e.g. stimulus size, viewing distance, duration of stimulus presentation), contribute to these inconsistencies (De Cesarei and Codispoti, 2013; Jeantet et al., 2018). In addition, also the behavioural task that is performed may influence the preferential use of specific SFs for (emotional) face processing, as diverse task demands may call for specific diagnostic cues, enveloped in certain SF ranges (Goffaux et al., 2003b; Schyns and Oliva, 1999; Smith and Merlusca, 2014). Furthermore, comparison across studies is also hampered by the use of different units to express the

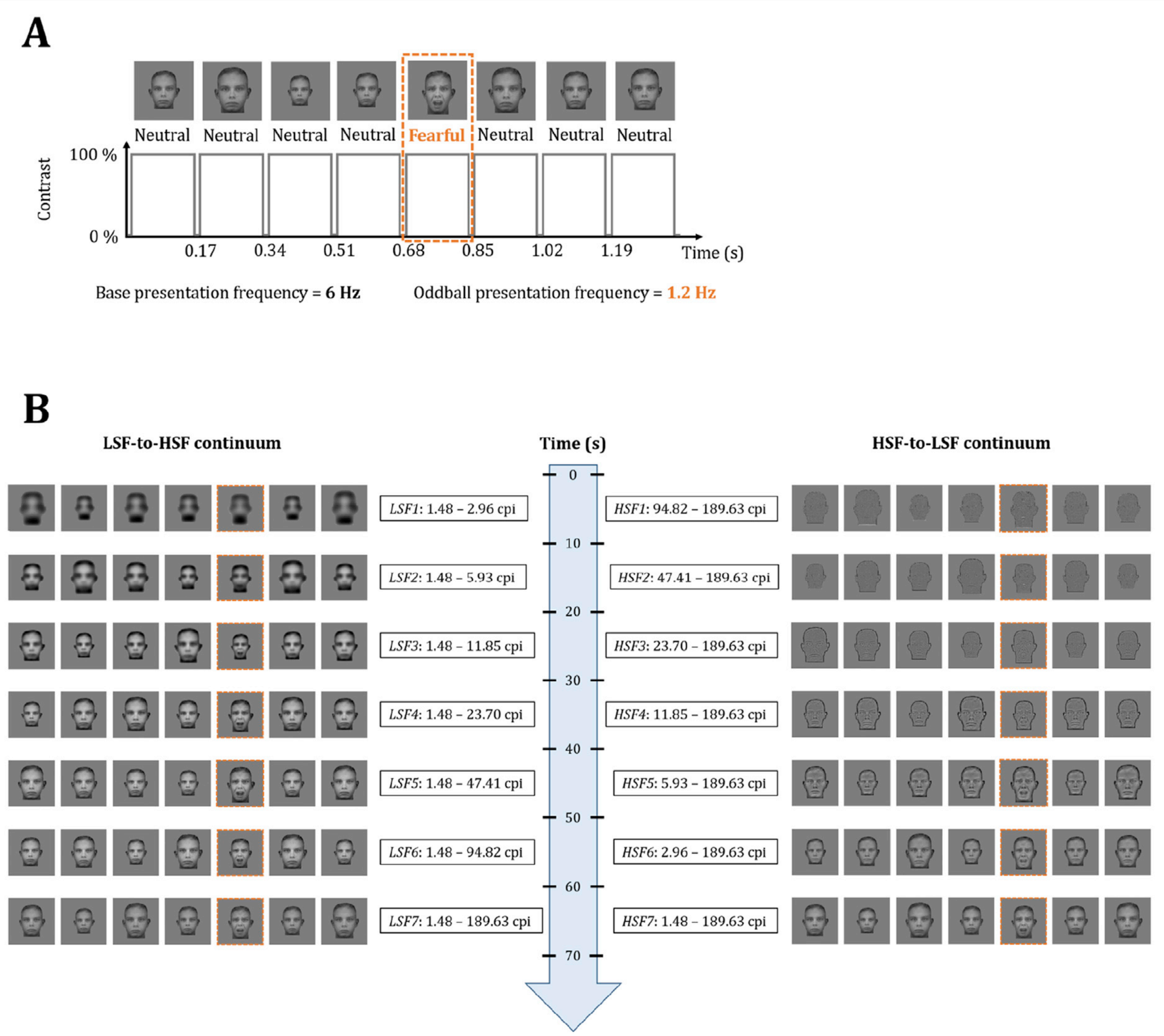

Fig. 1. A. Visualization of the square wave presentation of the experimental stimuli for a full SF spectrum face (i.e. SF 7). The stimulus sequence presented in each SF step: four neutral faces (base stimulus), followed by a fearful face (oddball stimulus). The base and oddball stimuli only differ in terms of facial expression; their SF content is identical. The placement of the fixation cross is not visualized. **B.** Examples of the seven logarithmic SF steps of the LSF-to-HSF and the HSF-to-LSF continua. Each SF step comprises 10 s of stimulus presentation, i.e. neutral faces periodically interleaved with fearful faces (every 5th image, i.e. 1.2 Hz). The stimuli of SF step 7 in both continua are identical, as they encompass the same SF range of 1.48–189.63 cpi. The original images were acquired from the KDEF database (Lundqvist et al., 1998) and adapted for experimental purposes.

SF content of the stimuli, as well as the use of highly variable cut-off values for demarcating the SF spectrum into LSFs, MSFs or HSFs (Jeantet et al., 2018). To move the field forward, ideally, the role of SF content on facial expression processing should be investigated in an implicit and automatic manner, without particular task demands that may modulate the impact or importance of particular SF content and without predefined and limited SF cut-offs, as explained next.

1.2. Present study

With the present study, we investigate the impact of SF content on the implicit neural detection of fearful faces among a series of rapidly presented neutral faces. We determine the minimally required SF information by systematically sweeping through a low-to-high and high-to-low SF space and employing a fast periodic visual stimulation (FPVS) oddball paradigm in combination with scalp electroencephalography (EEG). As in previous studies (Dzhelyova et al., 2017; Van der Donck et al., 2019), we present neutral faces at a fast periodic rate of 6 Hz, interleaved with expressive faces every 5th image, thus at 1.2 Hz oddball rate (see Fig. 1A). Here, we focus on fear detection, because of its evolutionary importance and its potential to elicit large neurophysiological responses (Nuske et al., 2014; Smith, 2012; Van der Donck et al., 2020). The periodic presentation at predefined, yet different, base and oddball frequency rates allows the direct quantification of the implicit neural responses, indicating the discrimination of fearful faces amongst neutral faces. In addition, the rapid presentation of the facial stimuli during this paradigm promotes automatic processing. By combining this implicit neural measure with an additional explicit fear-discrimination task (at the same presentation rate), we can investigate a possible differential use of SF information when processing facial expressions implicitly versus explicitly (Langner et al., 2012; Rohr and Wentura, 2014).

Based on a similar sweep paradigm addressing face categorization (Quek et al., 2018), we progressively increased the SF content of an image stream during 70 s, starting from a face image containing either only LSFs or only HSFs, until reaching the full spectrum with clearly recognizable neutral and fearful faces (see Fig. 1B/movies 1 and 2). The progressive changes of the SF filter cut-offs allow us to vary the SF content across a broad range throughout one stimulation sequence, without decomposing the images into discrete SF bands, thereby enabling the quantification of cumulative integration of facial expression information (Quek et al., 2018). Accordingly, this paradigm might allow us to pinpoint the threshold of optimal SF information for the rapid detection of fearful facial expressions, without prior assumptions about SF preferences.

Supplementary video related to this article can be found at https://doi.org/10.1016/j.neuroimage.2020.117151

Based on previous studies that demonstrated activity in higher-level face processing regions (e.g. fusiform gyrus) in response to LSF (Canário et al., 2016; Goffaux et al., 2011; Winston et al., 2003) as well as HSF faces (Goffaux et al., 2011; Rotshtein et al., 2007), we generally expect to see most brain activation over the left and right occipito-temporal regions.

As one may wonder to what extent our findings on preferred SF content are specific for facial fear detection and not merely for change detection in general (Morawetz et al., 2011), we added a control experiment where we inverted all the faces. While this manipulation preserves all low-level perceptual features, it has been well documented that face inversion typically disrupts holistic or configural face processing (Rossion, 2013; Tanaka and Farah, 1993; Vettori et al., 2019). Accordingly, we hypothesize that oddball responses will be lower for the inverted as compared to the upright faces. Previous studies have reported inversion effects for facial fear processing using FPVS oddball paradigms with full scale SF images (Dzhelyova et al., 2017; Van der Donck et al., 2019), but the inversion effect has also been observed in SF filtered faces. Most often, this face inversion effect has been reported in LSF faces (Flevaris et al., 2008; Goffaux, 2009; Goffaux and Rossion, 2006; Jeantet et al., 2018), suggesting that LSFs specifically contain the holistic or configural face information (Goffaux et al., 2005). Against this background, and given that HSFs comprise the facial features which are preserved during face inversion, we may expect a larger face inversion effect (i.e. lower fear-discrimination responses for inverted faces) for LSF versus HSF facial images. However, as configural relations between facial features can also be extracted on the basis of exclusive HSF information (Collin et al., 2014; Goffaux et al., 2005), we might also find a significant (but smaller) face inversion effect when only HSF information is present.

2. Methods

2.1. Participants

In the ***main experiment***, twenty right-handed healthy young adults (10 females) aged between 18 and 35 years old (mean age = 21.61 years, *SD* = 1.59) participated. One participant reported colour blindness, yet, because this did not affect the processing of the greyscale facial images or the detection of the colour-changes of the fixation cross, this participant was not excluded. In the ***control experiment***, we included a new group of ten healthy young adults (5 females; mean age = 26.48 years, *SD* = 3.21).

All participants reported normal or corrected-to-normal visual acuity. Given the "own-culture advantage" of emotion processing (Elfenbein and Ambady, 2002; Gendron et al., 2014), participants had to be living in Belgium or Europe for at least 5 years. An exclusion criterion was the diagnosis of epilepsy or autism spectrum disorder in the participant or in a first-degree relative. The Medical Ethical Committee of the university hospital approved this study. Written informed consent according to the Declaration of Helsinki was gathered from the participants prior to participation.

2.2. Stimuli

Full-frontal images of a neutral and fearful face of two male and two female actors were acquired from the Karolinska Directed Emotional Faces (KDEF) database (AF07, AF22, AM05, AM11 (Lundqvist et al., 1998)). Consulting the KDEF ratings, the most expressive faces were chosen in terms of reported arousal and intensity. All images were sized to 450 × 450 pixels and we removed the shoulders and stray hair, made the background transparent and centred the images on the nasion (i.e. the nose bridge). External features (e.g. hair and ears) were not removed, since this did not have an impact on the SF filtering. The stimuli were displayed subtending 6.01° visual angle at 80 cm viewing distance.

The broadband butterworth SF filtering (second order) of the images was performed using Matlab R2017b (The MathWorks, Inc.) and was based on the study of Petras et al. (2019). The full-spectrum neutral and fearful faces were first converted to greyscale and then bandpass filtered (i.e. by multiplying the Fourier amplitude of each image with the chosen SF filters, before transforming the stimuli back into image space) with seven logarithmic cut-offs (i.e. SF steps). This enabled us to investigate an entire range of SFs between 1.48 and 189.63 cpi (corresponding to approximately 0.66 and 84.46 cycles per face width (cpf), based on the mean cut-off estimate across the faces of the four actors). In two separate continua, we started from a stimulus with isolated LSF content or HSF content, where SF information was incrementally added throughout the seven SF steps, towards a stimulus containing the full spectrum (Fig. 1B). Henceforth, we will refer to these continua as the LSF-to-HSF continuum and the HSF-to-LSF continuum, respectively.

The resulting spatially filtered greyscale images were placed against a grey background (RGB = 128, 128, 128; alpha = 255) and equalized for contrast and luminance to match the mean values of the full-spectrum images. Consequently, per condition, all images had equal contrast and luminance, both within and across the seven SF steps, to ensure that only the facial expression differed between the base and oddball stimuli.

2.3. Design and procedure

Participants were seated in a dimly lighted room at 80 cm viewing distance of a LCD 24-in. computer screen. A custom application software written in Java was used to display the stimuli through square wave presentation, because the display time of the full contrast stimulus is much longer with a square wave presentation than sinusoidal contrast modulation. The 100% contrast stimulus presentation was approximately 167 ms (see Fig. 1A). To avoid detection of the fearful face due to low-level repetition effects, the stimuli varied randomly in size between 80% and 120% of the original size.

To guarantee attentiveness of the participants, an orthogonal task was implemented. A fixation cross, presented on the nasion of the face, briefly (300 ms) changed colour from black to red 10 times within every sequence. The participants had to press a button as soon and accurately as possible when noticing the colour changes of the fixation cross.

2.3.1. Implicit fear discrimination

In the ***main experiment***, the fear detection sweep paradigm consisted of 32 sequences in a randomized order with a sequence duration of 70 s. SF information was progressively added in seven logarithmic steps (10 s per SF step) within one sequence towards a stimulus containing the full SF-spectrum of 1.48–189.63 cpi (Fig. 1B). In the LSF-to-HSF continuum, the sequences started with a stimulus exclusively encompassing LSF information and each SF step added supplemental higher SF information. In contrast, the sequences of the HSF-to-LSF continuum started with a stimulus solely containing HSF information, adding lower SF information with each SF step. The sequence started and ended with a pre- and postlude step that functioned as a fade-in and a fade-out. This gradual start and end of each sequence was implemented to minimize artefacts due to the stimuli appearing or disappearing abruptly.

The 32 sequences comprised 16 LSF-to-HSF sequences (4 for each facial identity) and 16 HSF-to-LSF sequences (4 for each facial identity). This implies that every SF stimulus step was presented 16 times during a 10 s segment, totalling up to 160 s stimulation time, which is identical to the stimulation time used in previous (non-sweep) FPVS fear detection oddball paradigms (Dzhelyova et al., 2017; Van der Donck et al., 2019).

Within each sequence and within each SF step, neutral faces of one individual are presented at a base rate frequency of 6 Hz, periodically interleaved every fifth stimulus with a fearful face (oddball frequency of 1.2 Hz, i.e. 6 Hz/5) of the same individual. The only difference between the base (neutral faces) and oddball (fearful faces) stimuli is the facial expression; the SF content of the base and the oddball stimuli are identical (Fig. 1B). All images are presented upright.

In the ***control experiment***, we implemented a control condition where we, in addition to the sequences with the upright faces, also presented sequences with inverted faces. All other experimental parameters remained identical to the main experiment. Given that the main experiment showed that reliable fear-discrimination responses could already be obtained with half the number of stimulation sequences (i.e. 8 LSF-to-HSF and 8 HSF-to-LSF sequences), the control experiment only comprised 8 sequences per condition, resulting again in 32 sequences in total (based on both SF-continua and both orientations of the faces).

2.3.2. Explicit fear discrimination

Task demands have been found to modulate the use of particular SF information to enable fast stimulus processing (Awasthi et al., 2011; De Cesarei and Codispoti, 2013), while spontaneous SF processing without a specific visual task may shed light on the default SF components involved in implicit emotional face detection (Ruiz-Soler and Beltran, 2006). To investigate the mapping between implicit and explicit fear discrimination thresholds, we also administered an explicit behavioural fear detection task at the end of the test session.

For this task, again two sequences of the aforementioned fear detection sweep paradigm were shown: one sequence of the LSF-to-HSF continuum and one sequence of the HSF-to-LSF continuum, both displaying an individual of the same gender. Sequences displaying males or females were alternated for every participant. Here, participants had to press the response button once per sequence as soon as they detected a face with a fearful expression. Images were presented without a fixation cross, allowing the participants to look anywhere they wished on the computer screen.

2.4. EEG acquisition

We recorded EEG activity using a BIOSEMI Active-Two amplifier system with 64 Ag/AgCl electrodes and two additional electrodes as reference and ground electrodes (Common Mode Sense active electrode and Driven Right Leg passive electrode). Vertical eye movements were recorded via one electrode above and one below the right eye. One electrode was placed at the corner of both eyes to record horizontal eye movements. We recorded EEG and electrooculogram at 512 Hz. The electrode offset was kept under 30 μV.

2.5. EEG data analysis

Preprocessing. Similar to Quek et al. (2018), we processed all EEG data using Letswave 6 (http://www.nocions.org/letswave/) in Matlab R2017b (The Mathworks, Inc.). We cropped the data into segments of 75 s (3 s before and 2 s after each sequence), applied a fourth-order Butterworth bandpass filter (0.1–100 Hz) and resampled the data to 256 Hz. For four participants who blinked on average more than 15 times (based on robust Z-scores > 2.5 (Rousseeuw and Hubert, 2018)) within one sequence, we applied independent component analysis via the runica algorithm (Makeig et al., 1995) and removed the component that accounted for most of the variance. We re-estimated noisy or artifact-ridden channels through linear interpolation of the three spatially nearest, neighboring electrodes; on average across all participants, 1.42 electrodes were interpolated. All data segments were re-referenced to a common average reference and we averaged each participant's sequences for the LSF-to-HSF and HSF-to-LSF continua separately. The preprocessed data segments were then cropped according to each SF step (7×10 s segments).

Frequency-domain processing. Then, a fast Fourier transformation (FFT) was applied, yielding a spectrum between 0 and 127.84 Hz with a spectral resolution of 0.1 ($=1/10$s). In addition to the signal at the oddball and base frequencies, signals at frequencies corresponding to integer multiples (harmonics) of these base and oddball frequencies are also present in the spectrum. Only the amplitudes at the oddball frequency and its harmonics (i.e. $n*F/5 = 2.4$ Hz, 3.6 Hz, etc.) are considered as an index of facial expression discrimination (Dzhelyova et al., 2017). We used signal-to-noise ratio (SNR) and baseline-corrected amplitudes to describe these measures. SNR is calculated by dividing the amplitude value of a specific frequency bin by the average amplitude of the 8 surrounding frequency bins (Rossion et al., 2012). Baseline-corrected amplitudes are calculated by subtracting the average amplitude level of the 8 surrounding bins from the amplitude of the frequency bin of interest (Retter and Rossion, 2016). For both measures, these 8 surrounding bins are the 4 bins on each side of the target frequency bin, excluding the immediately neighboring bins and the two bins with the most extreme values, corresponding to a frequency range of 0.4 Hz. We used SNR spectra for visualization (see Fig. 2) because responses at high frequency ranges may be of small amplitude, but with a high SNR. Baseline correction expresses responses in amplitudes (μV) that can be summed across significant harmonics to quantify the overall base and oddball response (Retter and Rossion, 2016).

To estimate the number of informative oddball harmonics, we assessed the significance of the responses at different harmonics by calculating Z-scores – using the mean and standard deviation of the 8 frequency bins surrounding the bin of interest (Liu-Shuang et al., 2014) – on the FFT grand-averaged data across all electrodes and across electrodes in the relevant regions of interest (ROIs; cf. infra). Harmonics were

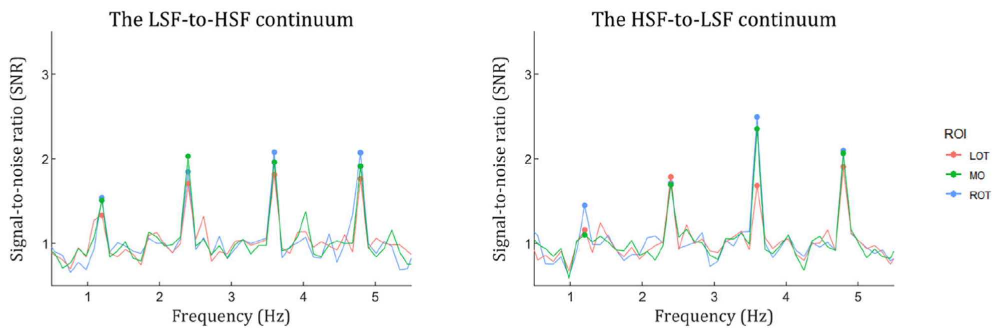

Fig. 2. SNR-spectra visualizing the fear-discrimination responses during SF step 7 in both continua, for the three ROIs separately. The significant first four harmonics are displayed.

considered significant and relevant to include as long as the Z-score for two consecutive harmonics was above 1.64 ($p < .05$, one-tailed) (Retter and Rossion, 2016). Following this principle, we quantified the oddball responses of the main and the control experiment as the sum of the oddball harmonics until the sixth harmonic following the first harmonic (i.e. 1.2 Hz), and the first four harmonics, respectively, excluding the harmonics corresponding to the base rate frequency.

Determination of ROIs. Visual inspection of the topographical maps and identification of the most responsive regions for emotional oddball stimulation (Dzhelyova et al., 2017; Van der Donck et al., 2019) led to three ROIs, identical for all paradigms. The left and right occipito-temporal (LOT and ROT) ROI were defined by averaging for each hemisphere the three channels with the highest summed baseline-corrected oddball response (i.e. channels P7, P9 and PO7 for LOT, and P8, P10 and PO8 for ROT). The medial-occipital ROI (MO) was defined by averaging the four channels with the largest common response at 6 Hz (i.e. channels Iz, Oz, O1 and O2).

2.6. Statistical data analysis

For statistical analyses of the baseline-corrected oddball amplitudes in each ROI, we applied a linear mixed-model (LMM) (function 'lmer' in R (Bates et al., 2015)), fitted with maximum likelihood. For both the main and the control experiment, a LMM was applied to the two SF conditions (LSF-to-HSF and HSF-to-LSF continua) separately, because main or interaction effects with this factor would not be of interest given the nature of the filtering parameters (Watier et al., 2010). *SF content* (seven SF steps) and *ROI* (LOT, ROT and MO) were included as fixed within-subject factors and a random intercept per participant to account for repeated testing. For the analysis of the control experiment, also *Orientation* (upright versus inverted) was included as a fixed within-subject factor. Degrees of freedom were calculated using the Kenward-Roger method. Posthoc contrasts were tested for significance using a Bonferroni correction for multiple comparisons, by multiplying the p-values by the number of comparisons. Cohen's *d* effect sizes were calculated by dividing the least square means difference by the pooled standard deviation. All assumptions in terms of linearity, normality and constant variance of residuals were verified and met for all LMMs.

For all analyses with EEG data, extreme outlying data points (based on a Cook's distance of more than six times the mean) were removed (Christensen et al., 1992). For one participant from the main experiment, data collection only included the LSF-to-HSF continuum. Consequently, analyses for the sweep FPVS oddball paradigm of the main experiment were conducted with data from 20 and 19 participants for the LSF-to-HSF continuum and HSF-to-LSF continuum, respectively.

Finally, a LMM was applied to ensure that the base and oddball responses for upright faces in the main and control experiment would not differ significantly, hence, indicating that the results in the control experiment can only be attributed to the orientation of the presented faces and not to underlying differences in this sample's response to upright faces.

For the behavioural data of the orthogonal task, we performed a Mann-Whitney *U* test.

17 of the 20 participants included in the main experiment performed the explicit behavioural task. Due to a missing value from one participant in each SF continuum, the data from 16 participants were analysed in both continua.

2.6.1. Fear detection threshold

As we aimed at pinpointing a neural detection threshold for the rapid discrimination of fearful faces amongst neutral faces, we evaluated the amount of SF content necessary for significant fear detection by calculating the 95% confidence interval around the group average fear-discrimination amplitude at each SF step (Quek et al., 2018). We interpreted the first SF step where the 95% confidence interval did not include zero as the fear-detection threshold, that is, the step where the discrimination response first emerged.

For the explicit fear discrimination task, we considered the SF step where at least half of the participants could detect the fearful face (i.e. the median value) as the most crucial cross-over point for behavioural fear detection.

3. Results

3.1. Explicit behavioural task

Fig. 3 provides a histogram displaying the number of participants that detected the fearful expression for each of the SF levels along the LSF-to-HSF and the HSF-to-LSF continuum. For the LSF-to-HSF continuum, the median detection level is situated at 3.5, which comprises SF3 and SF4 (max. range: 1.48 to 23.70 cpi, or 0.66 to 10.56 cpf). For the HSF-to-LSF continuum, the median of SF2 (SF range: 47.41 to 189.63 cpi, or 21.12 to 84.46 cpf) indicates that these images contained sufficient information to report detection of fearful faces.

3.2. Fixation cross change detection tasks

Results of the colour change detection tasks suggest similar levels of motivation and attention to the screen throughout both the main and the control experiment, across both continua and across upright and inverted faces, with equal accuracies (all $p > .22$) and reaction times (all $p > .44$) for all these conditions.

3.3. Fear-discrimination responses main experiment

The implicit, neural fear-discrimination responses, averaged across all participants, are visualized per SF step in Fig. 4.

3.3.1. LSF-to-HSF continuum

The LMM demonstrated a significant main effect of *SF content* (F(6,

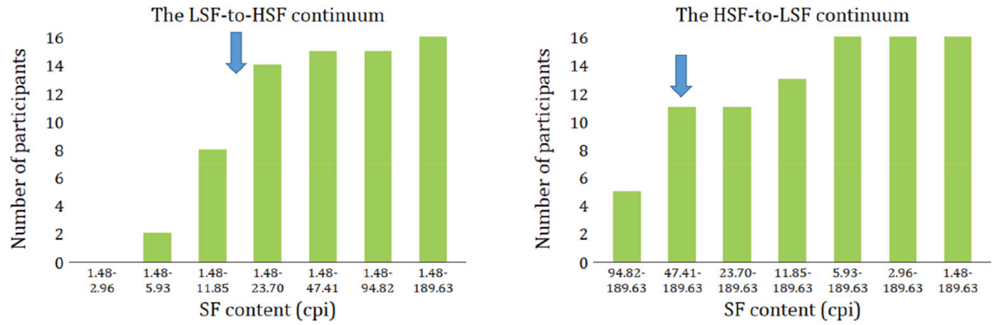

Fig. 3. The cumulative number of participants that explicitly detected the fearful expression for each of the SF levels along the LSF-to-HSF and the HSF-to-LSF continuum.

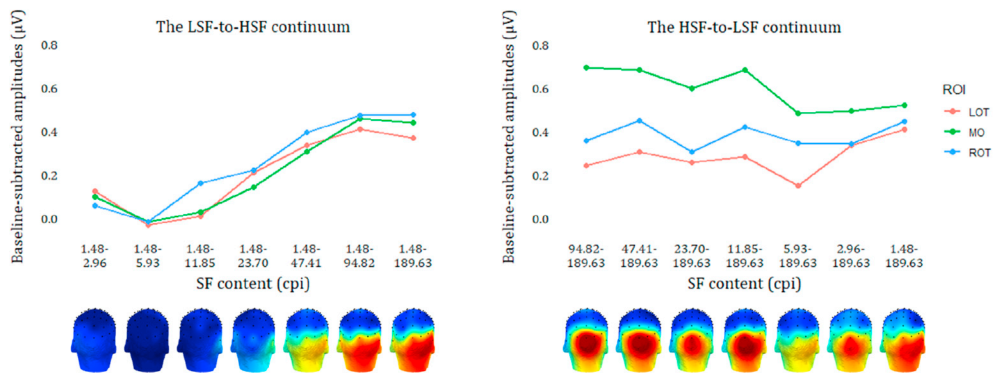

Fig. 4. Fear-discrimination responses for both continua during the main experiment, represented by the three identified ROIs (left and right occipito-temporal (LOT and ROT) and medial-occipital (MO) regions), with the corresponding topographies averaged across all participants.

367) = 45.07, $p < .0001$), with a significantly higher fear-discrimination response for LSF4 ($M_{LSF4} = 0.19$ µV) versus LSF2-3 ($M_{LSF2} = -0.02$ µV, $M_{LSF3} = 0.07$ µV; $t(367)_{LSF2\text{-}LSF4} = -5.47$, $d = -1{,}14$; $t(367)_{LSF3\text{-}LSF4} = -3.16$, $d = -0.59$; all $p_{Bonferroni} < .05$) and for LSF5-6-7 ($M_{LSF5} = 0.35$ µV, $M_{LSF6} = 0.45$ µV, $M_{LSF7} = 0.43$ µV) versus LSF1-2-3-4 ($M_{LSF1} = 0.09$ µV; $t(367)_{LSF1\text{-}LSF5} = -6.40$, $d = -1.18$; $t(367)_{LSF2\text{-}LSF5} = -9.31$, $d = -1.72$; $t(367)_{LSF3\text{-}LSF5} = -7.01$, $d = -1.19$; $t(367)_{LSF4\text{-}LSF5} = -3.88$, $d = -0.62$; $t(367)_{LSF1\text{-}LSF6} = -9.10$, $d = -1.52$; $t(367)_{LSF2\text{-}LSF6} = -12.01$, $d = -2.00$; $t(367)_{LSF3\text{-}LSF6} = -9.69$, $d = -1.51$; $t(367)_{LSF4\text{-}LSF6} = -6.56$, $d = -0.97$; $t(367)_{LSF1\text{-}LSF7} = -8.51$, $d = -1.38$; $t(367)_{LSF2\text{-}LSF7} = -11.39$, $d = -1.86$; $t(367)_{LSF3\text{-}LSF7} = -9.09$, $d = -1.39$; $t(367)_{LSF4\text{-}LSF7} = -6$, $d = -0.87$; all $p_{Bonferroni} \leq .01$). No other main or interaction effects were present (all $p > .08$, all $d < 0.17$).

3.3.2. HSF-to-LSF continuum

The LMM resulted in significant main effects of *SF content* ($F(6,352) = 2.50$, $p < .05$) and *ROI* ($F(2, 352) = 48.22$, $p < .0001$). Post hoc pairwise comparisons revealed highest responses in the MO compared to the LOT and ROT region, and significantly higher responses in the ROT versus LOT region ($M_{MO} = 0.59$ µV > $M_{ROT} = 0.38$ µV > $M_{LOT} = 0.28$ µV; $t(352)_{LOT\text{-}MO} = -9.66$, $d = 0.96$; $t(352)_{LOT\text{-}ROT} = -3.23$, $d = 0.36$; $t(352)_{MO\text{-}ROT} = 56.32$, $d = 0.66$; all $p_{Bonferroni} \leq .01$). In addition, we found a significantly lower fear discrimination response in HSF5 ($M_{HSF5} = 0.33$ µV), compared to HSF2 ($M_{HSF2} = 0.48$ µV; $t(352) = 3.11$, $d = 0.44$, $p < .05$). The interaction effect between these two factors was not significant ($p = .18$). All d for the non-significant findings were < 0.34.

3.4. Fear-discrimination control experiment with upright and inverted faces

Fig. 5 visualizes the implicit, neural fear-discrimination responses from the control experiment per SF step, averaged across all participants.

3.4.1. LSF-to-HSF continuum

The significant main effect of *Orientation* indicated higher fear-discrimination responses to upright ($M_{upright} = 0.20$ µV) versus inverted faces ($M_{inverted} = 0.05$ µV; $F(1,355) = 14.31$, $p = .0002$). This main

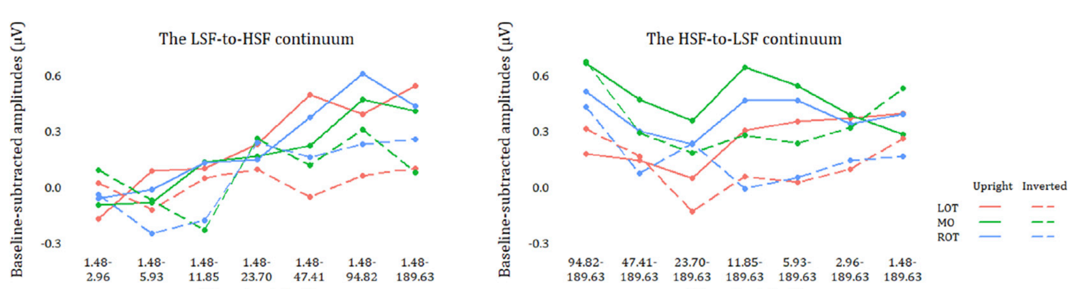

Fig. 5. Fear-discrimination responses for both continua during the control experiment, represented by the three identified ROIs (left and right occipito-temporal (LOT and ROT) and medial-occipital (MO) regions).

effect, and the main effect of *SF content* ($F(6,355) = 9.68$, $p < .0001$), were further qualified by their interaction ($F(6,355) = 2.47$, $p < .05$). For the upright faces, higher responses were elicited in LSF5-6-7 ($M_{LSF5} = 0.36$ μV, $M_{LSF6} = 0.49$ μV, $M_{LSF7} = 0.46$ μV) versus LSF1-2 ($M_{LSF1} = -0.11$ μV, $M_{LSF2} = -0.006$ μV; $t(355)_{LSF1\text{-}LSF5} = -4.32$, $d = -1.08$; $t(355)_{LSF2\text{-}LSF5} = -3.35$, $d = -0.79$; $t(356)_{LSF1\text{-}LSF6} = -5.17$, $d = -1.53$; $t(356)_{LSF2\text{-}LSF6} = -4.27$, $d = -1.17$; $t(355)_{LSF1\text{-}LSF7} = -5.19$, $d = -1.28$; $t(355)_{LSF2\text{-}LSF7} = -4.23$, $d = -0.98$; all $p_{Bonferroni} < .05$). Note that these findings are largely similar as in the main experiment with upright faces only. Yet, for the inverted faces there were no differences in response amplitude between stimulus pairs with different SF content (all $p > .09$, all d ranging between -0.23 and 0.14). In addition, the inversion effect (i.e. upright versus inverted face contrast) was only present for the HSF faces (i.e. LSF5-6-7, $p_{uncorrected} \leq .05$) and not for the LSF faces. There was no significant main effect of ROI, nor were there interactions with ROI (all $p > .43$, all d ranged between -0.13 and 0.13).

3.4.2. HSF-to-LSF continuum

For the data recorded during the control experiment, most importantly, we found a significant main effect of *Orientation* ($F(1,360) = 14.60$, $p = .0002$) showing that upright faces ($M_{upright} = 0.37$ μV) elicited larger fear-discrimination responses than the inverted faces ($M_{inverted} = 0.20$ μV, $d = 0.35$). Furthermore, the significant main effect of *SF content* ($F(6,360) = 2.65$, $p < .05$) indicated higher oddball responses for HSF1 versus HSF3 ($M_{HSF1} = 0.45$ μV, $M_{HSF3} = 0.14$ μV; $t(360) = 3.72$, $d = 0.68$, $p < .01$). Finally, we found significantly higher responses in the MO region versus the LOT and ROT region ($M_{MO} = 0.41$ μV, $M_{LOT} = 0.18$ μV, $M_{ROT} = 0.27$ μV; $t(360)_{Mo\text{-}LOT} = -4.52$, $d = 0.49$; $t(360)_{MO\text{-}ROT} = 2.80$, $d = 0.32$; all $p_{Bonferroni} < .05$). There were no significant interaction effects (all $p > .14$, all $d < 0.45$).

3.5. Determining the minimally required SF content for implicit neural fear-detection

We conducted two LMMs to investigate whether we could reliability pool the upright face data across the main and control experiment. Most importantly, for neither of both continua was there a main effect nor interaction effect with *Experiment* ($p > .50$, all $d < 0.13$), indicating the similarity of the upright fear-discrimination responses across both participant groups and confirming that data could reliably be combined for further analyses. Further, as expected, for the LSF-to-HSF continuum, there was the same main effect of *SF content* ($F(6,560) = 3.39$, $p = .003$) as described above. Similarly, for the HSF-to-LSF continuum, there was again the significant main effect of *ROI* ($F(2,549) = 8.82$, $p = .0002$), showing that highest responses were elicited over the MO region and lowest responses over the LOT region. No other main or interaction effects were significant, in neither of the LMMs (all $p > .05$).

Given that there are no significant differences between the fear-discrimination responses for upright faces in both experiments, we combined the results to increase the power for the identification of the fear-detection threshold. As displayed in Fig. 6, the fear-discrimination response almost linearly increased when systematically adding higher SF information to low SF images. The first SF step in the LSF-to-HSF continuum at which the average neural oddball response significantly differed from zero (i.e. the fear-detection threshold, defined as a 95% confidence interval that does not include zero), was located at LSF3 for the ROT region (i.e. 1.48 to 11.85 cpi, or 0.66 to 5.28 cpf) and at LSF4 for the LOT and MO regions (i.e. 1.48 to 23.70 cpi, or 0.66 to 10.56 cpf) (Fig. 6). Notably, for the inverted faces, none of the SF steps did reach the fear detection threshold level. When looking at the HSF-to-LSF continuum, on the other hand, we found that the first step with only the highest SF information already elicited clear oddball responses across the three ROIs and that increasing SF information by adding lower SFs did not enhance the responses. As is also evident from Fig. 6, indeed, the fear-discrimination threshold can already clearly be identified at HSF1 for all ROIs, indicating that the SF range of 94.82–189.63 cpi (or 42.23 to 84.46 cpf) already contains sufficient information to rapidly discriminate fearful faces from neutral faces.

4. Discussion

Against the background of a highly inconsistent and methodologically variable research field (Jeantet et al., 2018), we applied a FPVS sweep EEG paradigm to evaluate the optimal SF range to rapidly detect fearful faces. By systematically sweeping through an entire SF range, we explored which SF information is minimally required for the brain to detect briefly presented fearful expressions, without being constrained to predefined cut-offs for LSFs and HSFs.

4.1. Implicit neural fear discrimination mainly relies on HSFs

Although a LSF bias has been found for the categorization of fearful expressions (Pourtois et al., 2005; Vlamings et al., 2009; Vuilleumier et al., 2003), our results indicate a key role for HSFs during implicit neural fear discrimination. This is in line with previous research designating fear as a proximal expression that mostly employs higher SFs (Smith and Schyns, 2009). Our EEG data show that, indeed, automatic discrimination between neutral and fearful faces is impaired for LSF-filtered faces, compared to faces containing medium or higher SFs (Goren and Wilson, 2006). This echoes previous findings pinpointing the middle-to-high SF range as optimal for the processing of static expressions (Gao and Maurer, 2011; Plouffe-Demers et al., 2019; Stein et al., 2014). The detection threshold indicates that fearful faces need to comprise at least SF information between 1.48 and 11.85 cpi – corresponding with an SF range between 0.66 and 5.28 cpf – to be rapidly processed in terms of expression and to differentiate fearful from neutral

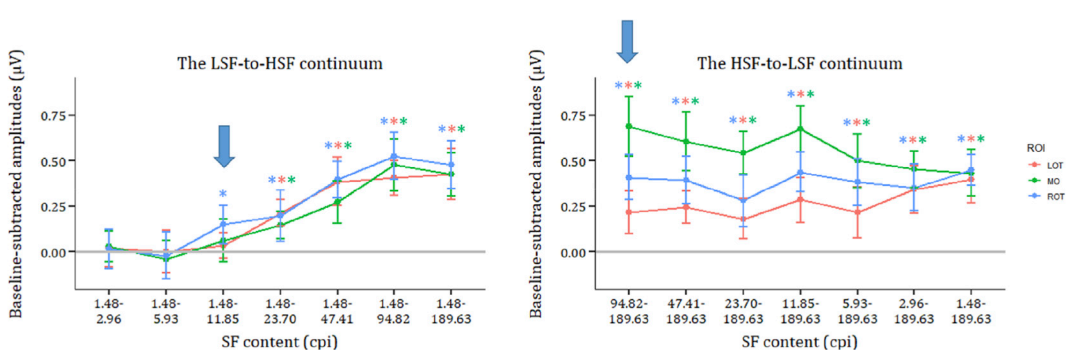

Fig. 6. Pinpointing the implicit neural fear-detection threshold across both SF continua, based on the 95% confidence interval around the mean amplitudes for each SF step. *Left:* In the LSF-to-HSF continuum, the fearful faces elicit significant neural responses in the ROT region at LSF3 (range: 1.48–11.85 cpi) and also in the MO and LOT regions at LSF4 (1.48–23.70 cpi). *Right:* In the HSF-to-LSF continuum, even HSF1 containing only HSFs (range: 94.82–189.63 cpi) already displays enough information to elicit significant fear-discrimination responses in each of the three ROIs. * indicate significant neural responses per ROI.

faces. Further adding higher SFs to a LSF face has a significant impact on the implicit neural sensitivity for rapidly presented fearful faces: it leads to an almost linear increase in the amplitude of the fear-discrimination responses. Moreover, the amplitude of the fear-discrimination response keeps increasing when adding higher SFs, even after reaching the initial detection threshold (i.e. the minimally required SF content to elicit a significant fear discrimination oddball response), possibly reaching a saturation plateau around LSF6-7 (cpi > 94.82, or cpf > 42.23), as the signal does not further increase. Possibly, this continuous accumulation of relevant higher SF information allows to progressively generate a (more accurate) visual representation of a fearful face, with its highly defined facial features and configural structure (Quek et al., 2018; Rotshtein et al., 2007), which facilitates the perceptual encoding. The right fusiform gyrus, involving the right fusiform face area, might play a key role in this process: it has been suggested that, here, LSF and HSF information received from separate cortical visual pathways is merged (Rotshtein et al., 2007). Although no exact source localization has been accomplished, it is notable that the ROT region is the first region to signal a significant fear detection threshold. Thus, the fear-discrimination responses in the ROT region were elicited already based on coarser information (LSF3) than those in the LOT and MO region (LSF4).

One may wonder to what extent our paradigm is effectively quantifying sensitivity for fearful expressions and not merely sensitivity to subtle featural perceptual changes. In this regard, it is important to emphasize that the oddball responses are robust despite the presence of continuous changes in stimulus size, thus they are not merely the result of low-level adaptation processes. More importantly, above all, the LSF-to-HSF continuum displays a significant Orientation x SF content interaction, indicating that the systematic increase in oddball responses as a result of adding more HSF content is only evident for the condition with the upright faces and not for the condition with the inverted faces. At the stimulus level, apart from being vertically flipped, low level features of the upright and inverted faces are identical, thus, apparently, they only differ at a perceptual level, with the upright faces being processed in a more configural manner, which increases the sensitivity for high-level facial expression differences. In a similar vein, comparing the significance of the fear detection thresholds in the upright versus inverted condition indicates that the face inversion effect is only present for stimuli comprising MSF to HSF information (i.e. only the MSF and HSF upright faces do show robust oddball fear discrimination responses). Previous studies, however, mostly reported detrimental inversion effects for faces containing only LSFs (Flevaris et al., 2008; Goffaux and Rossion, 2006; Jeantet et al., 2018), thereby suggesting that LSF faces may yield more configural information, which can be disturbed by the inversion operation. More recent studies, however, also reported face inversion effects across a wider range of SFs, including HSF faces (Gaspar et al., 2008; Royer et al., 2017; Willenbockel et al., 2010), thereby corroborating our findings.

Our EEG results contrast with the widespread notion that the processing of evolutionary relevant fearful faces may be driven by a fast subcortical process mainly making use of LSF visual information (Johnson, 2005), yet, it should not surprise that LSFs do not allow automatic fear detection with our oddball paradigm. Indeed, more recent studies have also cited the importance of HSF information in both the cortical and subcortical route for (rapid) fear processing (McFadyen et al., 2017; Pessoa and Adolphs, 2010; Stein et al., 2014).

Indeed, whereas images containing only LSFs did not enable successful discrimination of fearful faces among neutral faces, the results from the HSF-to-LSF continuum indicate that exclusive HSF faces, even in a restricted SF range between 94.82 and 189.63 cpi (i.e. HSF1; corresponding to 42.23 and 84.46 cpf), suffice to generate maximal fear-discrimination responses (as visualized in Fig. 6). This is in line with HSFs carrying more detailed and richer information than LSFs (Goffaux et al., 2005), and indicates that HSF1 already carries the critical information to extract the emotional expression of the faces (McBain et al., 2012; Quek et al., 2018). In fact, HSF1 may already carry *all* essential perceptual information to decode the emotional content of the stimulus, as adding lower SF information to the HSF images does not further boost the saliency of the oddball signal. Taken together across both continua, our results indicate that HSF information improves implicit fear discrimination when added to LSFs, and that HSF information by itself is sufficient to rapidly discriminate fearful faces. The presence of a significant inversion effect, also along the HSF-to-LSF continuum, ensures that the neural detection of the fearful faces is not merely driven by sensitivity to low-level perceptual changes. However, inspection of the response patterns for the HSF-to-LSF continuum suggests that these responses may be driven more strongly by basic stimulus characteristics. First, because the topographical distribution of the fear-discrimination responses is mainly centred around the MO region and is less lateralized towards face-selective ROT and LOT regions. Yet, this mostly medially activated topographical pattern for HSFs is in line with previous studies showing stronger activation in the MO region for stimuli containing higher SF information (Hemptinne et al., 2018; Henriksson et al., 2008; Tsuruhara et al., 2013) and suggests the extraction of basic visual properties of facial emotion expressions (Meaux and Vuilleumier, 2016). It seems as if the stimulus properties of HSF1 perfectly match with the tuning of neurons in the primary visual cortex (i.e. preference for higher SFs (e.g. Farivar et al., 2017; Sasaki et al., 2001; Singh et al., 2000)), and adding lower SF information immediately results in a reduction of this match (Shapley and Lennie, 1985) and consequently the oddball response, especially for the inverted faces. Second, because especially for HSF1, the face inversion effect is absent, suggesting that these fear detection responses are caused by low-level stimulus characteristics. However, facial emotion recognition has been found to rely on both local features and their global configuration, with varying roles of analytic and holistic information depending on the available information (Meaux and Vuilleumier, 2016; Tanaka et al., 2012). In addition, the visual system has been demonstrated to attend to the most informative scale (Schyns and Oliva, 1999; Sowden et al., 2003). Stimuli in HSF1 only contained very high SFs, hence, being the only informative scale that could be used, and in view of the EEG results, this edge-based information seemed to capture the structure of the facial cues that enable fear detection.

4.2. Explicit fear discrimination relies on a broader SF band

According to the flexible usage theory, the diagnostic SF information invoked for carrying out particular processes is dependent on the particular task demands (Morrison and Schyns, 2001; Oliva and Schyns, 1997; Ruiz-Soler and Beltran, 2006; Smith and Merlusca, 2014). Our results seem to support this. While the emotional expression of the faces can be detected based on a subset of SFs (De Cesarei and Codispoti, 2013), the diagnostic SF information differs slightly dependent whether fearful faces have to be discriminated implicitly versus explicitly. Analyses of the behavioural responses demonstrated that for the majority of the participants explicit fear discrimination emerged around LSF4 and HSF2, whereas the implicit fear-discrimination threshold was located one SF step earlier at LSF3 and HSF1, respectively. This indicates that explicit fear processing seems to require (a little bit) more SF information than the implicit neural encoding of fearful faces. By cumulatively increasing SF information in images containing either only low or only high SFs, the SF range is stretched towards the mid-SF band. Indeed, the mid-SF band, which carries both configural and featural information (Watier et al., 2010), has been found to be optimal for facial expression processing at the behavioural level (Gao and Maurer, 2011; Plouffe-Demers et al., 2019). Possibly, to decide with certainty whether fearful faces are really perceived, participants rely on a broader SF range that increases the visibility of the oddball stimuli.

The main objective of this study was to determine the minimally required SF information (i.e. identifying a detection threshold) for the rapid discrimination of fearful expressions in a series of neutral faces. However, given that the diagnostic information underlying facial expression categorization depends on the comparison categories (Smith and Merlusca, 2014), contrasting a given expression (other than fear) to neutrality or other facial expressions via this sweep FPVS oddball approach would be interesting. In addition, in order to reach our main objective, we equalized the contrast and luminance of the images both within and across the seven SF steps, to ensure that only the facial expression differed between the base and oddball stimuli. Contrast equalization alters the relative contrast of neutral and fearful facial stimuli (Webb and Hibbard, 2019), especially in HSF filtered images (Webb et al., preprint), which might have enhanced the energy of the HSFs. However, as previous findings indicated a LSF bias for fear processing, both in images with and without equalized contrast, despite a faster processing of HSF filtered fearful faces after contrast equalization, as compared to non-equalized images (Vlamings et al., 2009), we believe that our choices of filtering procedure did not inflate the importance of HSF information.

5. Conclusions

We applied a sweep FPVS oddball paradigm to investigate the minimally required SF information for rapid neural and behavioural fear discrimination. Results suggest that rapid and implicit fear detection mainly requires HSF information: HSFs have an additive beneficial value when added to images containing only LSF and HSF information by itself allows neural detection of fearful faces. However, a slightly broader SF range is involved in explicit fear detection. This suggests that rapid fear discrimination mainly relies on the optimal range of middle-to-high SFs.

Funding

This work was supported by two grants of the Research Foundation Flanders: grant G0C7816N, awarded to BB, and the Excellence of Science EOS grant G0E8718N (HUMVISCAT), awarded to JW and BB.

Declaration of competing interest

None.

CRediT authorship contribution statement

Stephanie Van der Donck: Conceptualization, Methodology, Validation, Formal analysis, Investigation, Writing - original draft. **Tiffany Tang:** Software, Validation, Formal analysis, Investigation, Resources, Writing - review & editing. **Milena Dzhelyova:** Conceptualization, Methodology, Writing - review & editing. **Johan Wagemans:** Conceptualization, Methodology, Writing - review & editing. **Bart Boets:** Conceptualization, Methodology, Validation, Writing - review & editing.

Acknowledgements

The authors would like to thank Kirsten Petras and Valérie Goffaux for their help with the spatial frequency filtering of the stimuli.

Appendix A. Supplementary data

Supplementary data to this article can be found online at https://doi.org/10.1016/j.neuroimage.2020.117151.

References

Awasthi, B., Friedman, J., Williams, M.A., 2011. Faster, stronger, lateralized: low spatial frequency information supports face processing. Neuropsychologia 49, 3583–3590. https://doi.org/10.1016/j.neuropsychologia.2011.08.027.

Bates, D., Maechler, M., Bolker, B., Walker, S., 2015. Package "lme4. J. Stat. Software 67, 1–48. https://doi.org/10.2307/2533043.

Canário, N., Jorge, L., Loureiro Silva, M.F., Alberto Soares, M., Castelo-Branco, M., 2016. Distinct preference for spatial frequency content in ventral stream regions underlying the recognition of scenes, faces, bodies and other objects. Neuropsychologia 87, 110–119. https://doi.org/10.1016/j.neuropsychologia.2016.05.010.

Christensen, R., Pearson, L.M., Johnson, W., 1992. Case-deletion diagnostics for mixed models. Technometrics 34, 38–45. https://doi.org/10.1080/00401706.1992.10485231.

Collin, C.A., Rainville, S., Watier, N., Boutet, I., 2014. Configural and featural discriminations use the same spatial frequencies: a model observer versus human observer analysis. Perception 43, 509–526. https://doi.org/10.1068/p7531.

Collin, C.A., Therrien, M.E., Campbell, K.B., Hamm, J.P., 2012. Effects of band-pass spatial frequency filtering of face and object images on the amplitude of N170. Perception 41, 717–732. https://doi.org/10.1068/p7056.

Costen, N.P., Parker, D.M., Craw, I., 1996. Effects of high pass and low pass spatial filtering on face identification. Percept. Psychophysiology 58, 602–612.

De Cesarei, A., Codispoti, M., 2013. Spatial frequencies and emotional perception. Rev. Neurosci. 24, 89–104. https://doi.org/10.1515/revneuro-2012-0053.

de Gardelle, V., Kouider, S., 2010. How spatial frequencies and visual awareness interact during face processing. Psychol. Sci. 21 https://doi.org/10.1177/0956797609354064, 58–56.

De Valois, R.L., De Valois, K.K., 1980. Spatial vision. Annu. Rev. Psychol. 31, 309–341. https://doi.org/10.1146/annurev.ps.31.020180.001521.

Dzhelyova, M., Jacques, C., Rossion, B., 2017. At a single glance: fast periodic visual stimulation uncovers the spatio-temporal dynamics of brief facial expression changes in the human brain. Cerebr. Cortex 1–18. https://doi.org/10.1093/cercor/bhw223.

Farivar, R., Clavagnier, S., Hansen, B.C., Thompson, B., Hess, R.F., 2017. Non-uniform phase sensitivity in spatial frequency maps of the human visual cortex. J. Physiol. 595, 1351–1363. https://doi.org/10.1113/JP273206.

Fiorentini, A., Maffei, L., Sandini, G., 1983. The role of high spatial frequencies in face perception. Perception 12, 195–201. https://doi.org/10.1068/p120195n.

Flevaris, A.V., Robertson, L.C., Bentin, S., 2008. Using spatial frequency scales for processing face features and face configuration: an ERP analysis. Brain Res. 1194, 100–109. https://doi.org/10.1016/j.brainres.2007.11.071.

Gao, X., Maurer, D., 2011. A comparison of spatial frequency tuning for the recognition of facial identity and facial expressions in adults and children. Vis. Resour. 51, 508–519. https://doi.org/10.1016/j.visres.2011.01.011.

Gaspar, C., Sekuler, A.B., Bennett, P.J., 2008. Spatial frequency tuning of upright and inverted face identification. Vis. Resour. 48, 2817–2826. https://doi.org/10.1016/j.visres.2008.09.015.

Goffaux, V., 2009. Spatial interactions in upright and inverted faces: Re-exploration of spatial scale influence. Vis. Resour. 49, 774–781. https://doi.org/10.1016/j.visres.2009.02.009.

Goffaux, V., Gauthier, I., Rossion, B., 2003a. Spatial scale contribution to early visual differences between face and object processing. Cognit. Brain Res. 16, 416–424. https://doi.org/10.1016/S0926-6410(03)00056-9.

Goffaux, V., Hault, B., Michel, C., Vuong, Q.C., Rossion, B., 2005. The respective role of low and high spatial frequencies in supporting configural and featural processing of faces. Perception 34, 77–86. https://doi.org/10.1068/p5370.

Goffaux, V., Jemel, B., Jacques, C., Rossion, B., Schyns, P.G., 2003b. ERP evidence for task modulations on face perceptual processing at different spatial scales. Cognit. Sci. 27, 313–325. https://doi.org/10.1016/S0364-0213(03)00002-8.

Goffaux, V., Peters, J.C., Haubrechts, J., Schiltz, C., Jansma, B., Goebel, R., 2011. From coarse to fine? spatial and temporal dynamics of cortical face processing. Cerebr. Cortex 21, 467–476. https://doi.org/10.1093/cercor/bhq112.

Goffaux, V., Rossion, B., 2006. Faces are "spatial"–holistic face perception is supported by low spatial frequencies. J. Exp. Psychol. Hum. Percept. Perform. 32, 1023–1039. https://doi.org/10.1037/0096-1523.32.4.1023.

Goren, D., Wilson, H.R., 2006. Quantifying facial expression recognition across viewing conditions. Vis. Resour. 46, 1253–1262. https://doi.org/10.1016/j.visres.2005.10.028.

Halit, H., de Haan, M., Schyns, P.G., Johnson, M.H., 2006. Is high-spatial frequency information used in the early stages of face detection? Brain Res. 1117, 154–161. https://doi.org/10.1016/j.brainres.2006.07.059.

Hegdé, J., 2008. Time course of visual perception: coarse-to-fine processing and beyond. Prog. Neurobiol. 84, 405–439. https://doi.org/10.1016/j.pneurobio.2007.09.001.

Hemptinne, C., Liu-Shuang, J., Yuksel, D., Rossion, B., 2018. Rapid objective assessment of contrast sensitivity and visual acuity with sweep visual evoked potentials and an extended electrode array. Investig. Ophthalmol. Vis. Sci. 59, 1144–1157. https://doi.org/10.1167/iovs.17-23248.

Henriksson, L., Nurminen, L., Hyvärinen, A., Vanni, S., 2008. Spatial frequency tuning in human retinotopic visual areas. J. Vision2 8. https://doi.org/10.1167/8.10.5.Introduction.

Holmes, A., Green, S., Vuilleumier, P., 2005. The involvement of distinct visual channels in rapid attention towards fearful facial expressions. Cognit. Emot. 19, 899–922. https://doi.org/10.1080/02699930441000454.

Jeantet, C., Caharel, S., Schwan, R., Lighezzolo-Alnot, J., Laprevote, V., 2018. Factors influencing spatial frequency extraction in faces: a review. Neurosci. Biobehav. Rev. 93, 123–138. https://doi.org/10.1016/j.neubiorev.2018.03.006.

Johnson, M.H., 2005. Subcortical face processing. Nat. Rev. Neurosci. 6, 766–774. https://doi.org/10.1038/nrn1766.

Keil, M.S., 2008. Does face image statistics predict a preferred spatial frequency for human face processing? Proc. R. Soc. B Biol. Sci. 275, 2095–2100. https://doi.org/10.1098/rspb.2008.0486.

Langner, O., Becker, E.S., Rinck, M., 2012. Higher sensitivity for low spatial frequency expressions in social anxiety: evident in indirect but not direct tasks? Emotion 12, 847–851. https://doi.org/10.1037/a0028761.

Leonard, H.C., Karmiloff-Smith, A., Johnson, M.H., 2010. The development of spatial frequency biases in face recognition. J. Exp. Child Psychol. 106, 193–207. https://doi.org/10.1016/j.jecp.2010.03.005.

Liu-Shuang, J., Norcia, A.M., Rossion, B., 2014. An objective index of individual face discrimination in the right occipito-temporal cortex by means of fast periodic oddball stimulation. Neuropsychologia 52, 57–72. https://doi.org/10.1016/j.neuropsychologia.2013.10.022.

Lundqvist, D., Flykt, A., Öhman, A., 1998. The Karolinska Directed Emotional Faces - KDEF. CD ROM from Department of Clinical Neuroscience, Psychology section.

Makeig, S., Bell, A.J., Jung, T.-P., Sejnowski, T.J., 1995. Independent component analysis of electroencephalographic data. In: Touretzky, D.S., Mozer, M.C., Hasselmo, M.E. (Eds.), Advances in Neural Information Processing Systems 8. MIT Press, Cambridge (MA), pp. 145–151.

McBain, R., Norton, D., Chen, Y., 2012. Differential spatial frequency modulations on facial emotion detection and perception. Open Behav. Sci. J. 6, 1–7. https://doi.org/10.2174/1874230001206010001.

McFadyen, J., Mermillod, M., Mattingley, J.B., Halász, V., Garrido, M.I., 2017. A rapid subcortical amygdala route for faces irrespective of spatial frequency and emotion. J. Neurosci. 37, 3864–3874. https://doi.org/10.1523/JNEUROSCI.3525-16.2017.

Meaux, E., Vuilleumier, P., 2016. Facing mixed emotions: analytic and holistic perception of facial emotion expressions engages separate brain networks. Neuroimage 141, 154–173. https://doi.org/10.1016/j.neuroimage.2016.07.004.

Morawetz, C., Baudewig, J., Treue, S., Dechent, P., 2011. Effects of spatial frequency and location of fearful faces on human amygdala activity. Brain Res. 1371, 87–99. https://doi.org/10.1016/j.brainres.2010.10.110.

Morrison, D.J., Schyns, P.G., 2001. Usage of spatial scales for the categorization of faces, objects, and scenes. Psychon. Bull. Rev. 8, 454–469. https://doi.org/10.3758/BF03196180.

Nuske, H.J., Vivanti, G., Dissanayake, C., 2014. Reactivity to fearful expressions of familiar and unfamiliar people in children with autism : an eye-tracking pupillometry study. J. Neurodev. Disord. 6.

Oliva, A., Schyns, P.G., 1997. Coarse blobs or fine edges? Evidence that information diagnosticity changes the perception of complex visual stimuli. Cognit. Psychol. 34, 72–107. https://doi.org/10.1006/cogp.1997.0667.

Pessoa, L., Adolphs, R., 2010. Emotion processing and the amygdala: from a 'low road' to 'many roads' of evaluating biological significance. Nat. Rev. Neurosci. 11, 773–783. https://doi.org/10.1038/nrn2920.

Petras, K., ten Oever, S. ten, Jacobs, C., Goffaux, V., 2019. Coarse-to-fine information integration in human vision. Neuroimage 186, 103–112. https://doi.org/10.1016/j.neuroimage.2018.10.086.

Plouffe-Demers, M.-P., Fiset, D., Saumure, C., Duncan, J., Blais, C., 2019. Strategy shift toward lower spatial frequencies in the recognition of dynamic facial expressions of basic emotions: when it moves it is different. Front. Psychol. 10 https://doi.org/10.3389/fpsyg.2019.01563.

Pourtois, G., Dan, E.S., Grandjean, D., Sander, D., Vuilleumier, P., 2005. Enhanced extrastriate visual response to bandpass spatial frequency filtered fearful faces: time course and topographic evoked-potentials mapping. Hum. Brain Mapp. 26, 65–79. https://doi.org/10.1002/hbm.20130.

Quek, G.L., Liu-Shuang, J., Goffaux, V., Rossion, B., 2018. Ultra-coarse, single-glance human face detection in a dynamic visual stream. Neuroimage 176, 465–476. https://doi.org/10.1016/j.neuroimage.2018.04.034.

Retter, T.L., Rossion, B., 2016. Uncovering the neural magnitude and spatio-temporal dynamics of natural image categorization in a fast visual stream. Neuropsychologia 91, 9–28. https://doi.org/10.1016/j.neuropsychologia.2016.07.028.

Rohr, M., Wentura, D., 2014. Spatial frequency filtered images reveal differences between masked and unmasked processing of emotional information. Conscious. Cogn 29, 141–158. https://doi.org/10.1016/j.concog.2014.08.021.

Rossion, B., 2013. The Composite Face Illusion: A Whole Window into Our Understanding of Holistic Face Perception. Vis. cogn. https://doi.org/10.1080/13506285.2013.772929.

Rossion, B., Prieto, E.A., Boremanse, A., Kuefner, D., Van Belle, G., 2012. A steady-state visual evoked potential approach to individual face perception: Effect of inversion, contrast-reversal and temporal dynamics. NeuroImage 63, 1585–1600. https://doi.org/10.1016/j.neuroimage.2012.08.033.

Rotshtein, P., Vuilleumier, P., Winston, J., Driver, J., Dolan, R., 2007. Distinct and convergent visual processing of high and low spatial frequency information in faces. Cerebr. Cortex 17, 2713–2724. https://doi.org/10.1093/cercor/bhl180.

Rousseeuw, P.J., Hubert, M., 2018. Anomaly detection by robust statistics. WIREs Data Min. Knowl Discov. https://doi.org/10.1002/widm.1236.

Royer, J., Willenbockel, V., Blais, C., Gosselin, F., Lafortune, S., Leclerc, J., Fiset, D., 2017. The influence of natural contour and face size on the spatial frequency tuning for identifying upright and inverted faces. Psychol. Res. 81, 13–23. https://doi.org/10.1007/s00426-015-0740-3.

Ruiz-Soler, M., Beltran, F.S., 2006. Face perception: an integrative review of the role of spatial frequencies. Psychol. Res. 70, 273–292. https://doi.org/10.1007/s00426-005-0215-z.

Sasaki, Y., Hadjikhani, N., Fischl, B., Liu, A.K., Marret, S., Dale, A.M., Tootell, R.B.H., 2001. Local and global attention are mapped retinotopically in human occipital cortex. Proc. Natl. Acad. Sci. U.S.A. 98, 2077–2082. https://doi.org/10.1073/pnas.98.4.2077.

Schyns, P.G., Oliva, A., 1999. Dr. Angry and Mr. Smile: when categorization flexibly modifies the perception of faces in rapid visual presentations. Cognition 69, 243–265. https://doi.org/10.1016/S0010-0277(98)00069-9.

Shapley, R., Lennie, P., 1985. Spatial frequency analysis in the visual system. Annu. Rev. Neurosci. 8, 547–581. https://doi.org/10.1146/annurev.ne.08.030185.002555.

Singh, K.D., Smith, A.T., Greenlee, M.W., 2000. Spatiotemporal frequency and direction sensitivities of human visual areas measured using fMRI. Neuroimage 12, 550–564. https://doi.org/10.1006/nimg.2000.0642.

Smith, F.W., Schyns, P.G., 2009. Smile through your fear and sadness. Psychol. Sci. 20, 1202–1208. https://doi.org/10.1111/j.1467-9280.2009.02427.x.

Smith, M.L., 2012. Rapid processing of emotional expressions without conscious awareness. Cerebr. Cortex 22, 1748–1760. https://doi.org/10.1093/cercor/bhr250.

Smith, M.L., Merlusca, C., 2014. How task shapes the use of information during facial expression categorizations. Emotion 14, 478–487. https://doi.org/10.1037/a0035588.

Sowden, P.T., Özgen, E., Schyns, P.G., Daoutis, C., 2003. Expectancy effects on spatial frequency processing. Vis. Resour. 43, 2759–2772. https://doi.org/10.1016/S0042-6989(03)00480-2.

Stein, T., Seymour, K., Hebart, M.N., Sterzer, P., 2014. Rapid fear detection relies on high spatial frequencies. Psychol. Sci. 25, 566–574. https://doi.org/10.1177/0956797613512509.

Tanaka, J.W., Farah, M.J., 1993. Parts and wholes in face recognition. Q. J. Exp. Psychol. 46A, 225–245. https://doi.org/10.1016/0257-8972(91)90292-5.

Tanaka, J.W., Kaiser, M.D., Butler, S., Le Grand, R., 2012. Mixed emotions: holistic and analytic perception of facial expressions. Cognit. Emot. 26, 961–977. https://doi.org/10.1080/02699931.2011.630933.

Tsuruhara, A., Nagata, Y., Suzuki, M., Inui, K., Kakigi, R., 2013. Effects of spatial frequency on visual evoked magnetic fields. Exp. Brain Res. 226, 347–355. https://doi.org/10.1007/s00221-013-3440-5.

Van der Donck, S., Dzhelyova, M., Vettori, S., Mahdi, S.S., Claes, P., Steyaert, J., Boets, B., 2020. Rapid neural categorization of angry and fearful faces is specifically impaired in boys with autism spectrum disorder. J. Child Psychol. Psychiatry. https://doi.org/10.1111/jcpp.13201.

Van der Donck, S., Dzhelyova, M., Vettori, S., Thielen, H., Steyaert, J., Rossion, B., Boets, B., 2019. Fast periodic visual stimulation EEG reveals reduced neural sensitivity to fearful faces in children with autism. J. Autism Dev. Disord. 49, 4658–4673. https://doi.org/10.1007/s10803-019-04172-0.

Vettori, S., Dzhelyova, M., Van der Donck, S., Jacques, C., Steyaert, J., Rossion, B., Boets, B., 2019. Reduced neural sensitivity to rapid individual face discrimination in autism spectrum disorder. NeuroImage Clin 21. https://doi.org/10.1016/j.nicl.2018.101613.

Vlamings, P.H.J.M., Goffaux, V., Kemner, C., 2009. Is the early modulation of brain activity by fearful facial expressions primarily mediated by coarse low spatial frequency information? J. Vis. 9 https://doi.org/10.1167/9.5.12, 12–12.

Vuilleumier, P., Armony, J.L., Driver, J., Dolan, R.J., 2003. Distinct spatial frequency sensitivities for processing faces and emotional expressions. Nat. Neurosci. 6, 624–631. https://doi.org/10.1038/nn1057.

Wang, S., Eccleston, C., Keogh, E., 2015. The role of spatial frequency information in the recognition of facial expressions of pain. Pain. https://doi.org/10.1097/j.pain.0000000000000226.

Watier, N., Collin, C.A., Boutet, I., 2010. Spatial-frequency thresholds for configural and featural discriminations in upright and inverted faces. Perception 39, 502–513. https://doi.org/10.1068/p6504.

Webb, A.L.M., Hibbard, P.B., 2019. The effect of facial expression on contrast sensitivity: a behavioural investigation and extension of Hedger, Adams & Garner (2015). PloS One 14, 1–18. https://doi.org/10.1371/journal.pone.0205621.

Webb, A.L.M., Hibbard, P.B., O'Gorman, R., n.d. Contrast normalisation masks natural expression-related differences and artificially enhances the perceived salience of fear expressions. https://doi.org/10.11164/jjsps.8.2_255_5.

Willenbockel, V., Fiset, D., Chauvin, A., Blais, C., Arguin, M., Tanaka, J.W., Bub, D.N., Gosselin, F., 2010. Does face inversion change spatial frequency tuning? J. Exp. Psychol. Hum. Percept. Perform. 36, 122–135. https://doi.org/10.1037/a0016465.

Winston, J.S., Vuilleumier, P., Dolan, R.J., 2003. Effects of low-spatial frequency components of fearful faces on fusiform cortex activity. Curr. Biol. 13, 1824–1829. https://doi.org/10.1016/j.cub.2003.09.038.